Chapter 7

Two-Photon Optogenetic Stimulation of *Drosophila* Neurons

Mehmet Fişek and James M. Jeanne

Abstract

Optogenetics enables experimental control over neural activity using light. Channelrhodopsin and its variants are typically activated using visible light excitation but can also be activated using infrared two-photon excitation. Two-photon excitation can improve the spatial precision of stimulation in scattering tissue but has several practical limitations that need to be considered before use. Here we describe the methodology and best practices for using two-photon optogenetic stimulation of neurons within the brain of the fruit fly, *Drosophila melanogaster*, with an emphasis on projection neurons of the antennal lobe.

Key words Optogenetics, Two-photon microscopy, *Drosophila melanogaster*, Neural circuits, Neural coding

1 Introduction

Optogenetic tools such as channelrhodopsin enable millisecond-timescale activation and silencing of neurons with cell-type specificity in intact living brains [1]. Traditional one-photon excitation strategies are generally limited to controlling neural activity in a large number of neurons because excitation light cannot selectively target volumes as small as single cells in neural tissue. Two-photon excitation overcomes this limitation through the nonlinear interactions of light with matter, achieving subcellular spatial resolution [2].

Channelrhodopsin has a large two-photon cross section [i.e., relatively small amounts of light are needed to open the channel; 3]. However, each molecule has a small single-channel conductance. This means that many channels need to open in order to drive substantial neuronal depolarization [e.g., to evoke spikes; 3, 4]. The high spatial precision of two-photon excitation therefore necessitates careful spatiotemporal control of light to ensure sufficient illumination of target cells while avoiding illumination of off-target cells.

Robert E. Dempski (ed.), *Channelrhodopsin: Methods and Protocols*, Methods in Molecular Biology, vol. 2191,
https://doi.org/10.1007/978-1-0716-0830-2_7,

Multiple avenues for improving the spatiotemporal resolution, efficiency of stimulation, and the flexibility of this technique are being pursued in this rapidly advancing field. The engineering of new opsins can improve multiphoton excitation efficiency [5]. Shifting excitation spectra can allow independent control over distinct targets using different wavelengths [6]. Restricted expression in subcellular compartments can improve effective spatial resolution of stimulation [5]. Sophisticated light-sculpting methods can target complex shapes and locations in the brain [7]. Imaging of cellular activity can be performed simultaneously with stimulation to obtain closed-loop control [8]. These advances illustrate the promise for the future of two-photon optogenetics.

The fruit fly, *Drosophila melanogaster*, is widely used for circuit and systems neuroscience. This is due, in large part, to its numerically compact brain, stereotypy of neuronal connectivity and function, and the ability to perform electrical and optical recordings from genetically defined neurons [9]. Like the brains of other animals, the fruit fly brain is organized into discrete neuropils that perform distinct functions [10]. A few neuropils in the fly brain are especially structured, with a close correspondence between structure and cell type. Examples of these structured neuropils include the antennal lobe, the mushroom body, the central complex, the optic lobes, and optic glomeruli.

In many species, two-photon optogenetic stimulation targeted directly to neuronal somata can achieve single-cell resolution [e.g. Ref. 5]. In the fly, this approach is not as effective, because spike initiation sites are often distant from the soma [11]. Stimulation of the structured neuropil in the fly brain, however, offers considerable advantages for two-photon optogenetics. First, because the dendritic arbors of different neurons innervate different regions of space, single-cell, or near-single-cell resolution can be obtained with genetic driver lines that target entire cell classes [e.g., Ref. 12]. Second, since dendritic processes are a major site for signal integration leading to spikes [11], they are effective targets for optogenetic photostimulation. Third, the dense and compact dendritic morphology provides a high surface area to volume ratio, localizing many membrane-bound channels into a small volume that is compatible with the small two-photon excitation volumes. To date, two-photon optogenetic stimulation has primarily been applied to neurons of structured neuropils. These include the antennal lobe [13, 14], central complex [15], and the larval ventral nerve cord [16], but *see also* [17].

In this chapter, we describe methods and best practices for two-photon optogenetic stimulation of *Drosophila* neurons. Our focus is on ex vivo strategies to stimulate dendrites of projection neurons in the antennal lobe, a well-characterized and highly structured neuropil. However, these stimulation strategies and associated methods can apply to stimulation of any neuron or

neuron class that can selectively express an optogenetic actuator ex vivo or in vivo. Because it is important to ensure that stimulation activates the intended neurons, and none of the unintended neurons, we also describe methods for validating activation parameters. These will need to be tuned for each individual microscope.

2 Materials

2.1 Major Equipment

- Two-photon laser scanning microscope with two independent galvonometric scan mirrors and piezoelectric actuator for fast objective movements.
- High numerical aperture (NA) and long working distance objective (e.g., Olympus XLUMPLFLN 20X 1.0NA).
- Femtosecond pulsed laser tunable to 1040 nm or above. Many commercially available excitation light sources are appropriate for two-photon optogenetics in *Drosophila*, including high repetition rate lasers classically used for two-photon imaging, like the Spectra-Physics MaiTai or the Coherent Chameleon Ultra. In addition, lower repetition rate, higher pulse energy lasers may be necessary under more extreme scattering conditions, as used in [17].
- Patch-clamp electrophysiology equipment, including amplifier, motorized manipulator, and digital acquisition board. Details of this equipment have been described elsewhere [18].
- Computer running ScanImage (scanimage.vidriotechnologies.com) [19], with appropriate data acquisition hardware.
- Power meter (e.g., ThorLabs PM100D), post-objective sensor head (e.g., ThorLabs S175C), and fluorescent microspheres (e.g., Invitrogen FocalCheck F36909) for alignment and calibration.

2.2 Consumable Materials

- Appropriate transgenic effector fly strains to express a channelrhodopsin variant of choice. UAS-ReaChR [20, 21] has been used successfully in the adult antennal lobe [13, 14]. UAS-CsChrimson [6] has been used successfully in the adult central complex [15]. Both are good choices and can be obtained from the Bloomington *Drosophila* Stock Center.
- Selective driver lines (e.g., of the Gal4 or LexA binary expression systems) to spatially restrict expression of optogenetic actuator [12]. Here we use *GH146-Gal4* [22] to label most projection neurons (PNs) of the antennal lobe.
- All-*trans*-retinal (ATR), a light-isomerizable chromophore, is necessary for proper function of all optogenetic actuators. Since this chromophore does not naturally exist in invertebrates

at sufficiently high levels, it must be supplemented in their food. A stock solution of 35 mM ATR in ethanol can be stored in the freezer for periodic use.

- Dissection forceps, sharpened to a fine point [23].
- Sylgard 184 clear silicone elastomer and curing agent.
- 50-μm-diameter tungsten wire.
- Internal and external saline for patch clamping [18, 23]. The external saline should contain 103 mM NaCl, 3 mM KCl, 5 mM *N-tris*(hydroxymethyl) methyl-2-aminoethane-sulfonic acid, 8 mM trehalose, 10 mM glucose, 26 mM $NaHCO_3$, 1 mM NaH_2PO_4, 1.5 mM $CaCl_2$, and 4 mM $MgCl_2$. The internal saline should contain 140 mM potassium aspartate, 10 mM 4-(2-hydroxyethyl)-1-piperazineethanesulfonic acid, 4 mM MgATP, 0.5 mM Na_3GTP, 1 ethylene glycol tetraacetic acid, 1 KCl, 13 biocytin hydrazide. Adding 50 μM Alexa Fluor 568 to your internal saline will enable online visualization of your recorded neuron if the two-photon microscope has a second PMT channel for red dyes.
- α-Bungarotoxin conjugated to Alexa Fluor 488 diluted to 116 μM in *Drosophila* external saline.

3 Methods

3.1 Prepare Flies

1. Depending on the nature of the experiment, the crosses necessary for producing the experimental fly will vary. Minimally, a driver line (e.g., *GH146-Gal4*) must be crossed to an opsin reporter line (e.g., *UAS-ReaChR*). We describe here an approach using ReaChR tagged with the fluorescent reporter mCitrine. An additional driver line may be needed to label potential postsynaptic neurons of interest. This will mean a three-generation cross at a minimum, requiring ~6 weeks advanced planning.
2. Harvest virgin flies into food vials supplemented with 200 μL of 35 mM ATR in ethanol. Maintain flies on ATR for at least 24 h (*see* **Note 1**).
3. Age flies. Patch-clamp recording is easier in younger flies, but they have lower transgene expression. Depending on the strength of the driver line, the best age will be anywhere between 1 and 4 days old.

3.2 Prepare Ex Vivo Recording Chamber and Micro-Dissection Pins

1. Mix Sylgard silicone elastomer and curing agent at a ratio of 9:1 in a 20 mm Petri dish to be fit onto a recording platform. Cure on a hot plate at lowest heat setting for 1–2 h or overnight (*see* **Note 2**). As an alternative to the Petri dish, a chamber can also

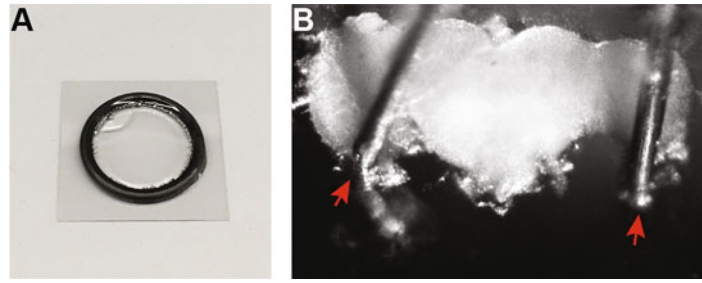

Fig. 1 Ex vivo brain preparation. (**a**) A small Sylgard chamber for mounting ex vivo *Drosophila* brains. A size 016 o-ring is glued to the surface of a 25 mm glass coverslip. The space inside the o-ring is filled with heat-cured Sylgard. (**b**) Photograph of a *Drosophila* brain pinned into the Sylgard chamber with tungsten micro-dissection pins (red arrows). Dissection pins are placed over the optic lobes, located on the lateral edges of the brain. This configuration leaves the antennal lobes (near the midline of the brain) unobscured for photostimulation and patch-clamp recording

be made by gluing an O-ring to a 25 mm glass coverslip (Fig. 1a).

2. Make micro-dissection pins by sharpening 50 μm tungsten wire using electrolysis (similar techniques have been described previously [24]). Repeatedly dip wire into saturated potassium nitrate solution while passing AC current through it using an adjustable voltage transformer (e.g., Variac). This should be performed in a fume hood for safety purposes.
3. Cut sharpened tungsten wire down to ~500 μm length and bend into an L-shape under a high magnification stereomicroscope using coarse forceps.
4. Stab tungsten pins into Sylgard and affix Petri dish to recording platform (*see* **Note 3**).

3.3 Prepare Microscope

1. Measure power output from the laser (at 1040 nm excitation wavelength) after the objective to confirm stability of excitation light. Perform this every day.
2. Check laser beam alignment into the microscope. Perform periodically and align if needed.
3. Measure effective excitation volume (point spread function) using submicron fluorescent microspheres. Ensure it is reasonably close to that expected for your system. Perform this step after every laser beam alignment (*see* **Note 4**).

3.4 Dissect Brain

The description here is provided for an ex vivo brain dissection. Description of in vivo dissection and preparation is provided in [23]:

1. Submerge fly under extracellular saline, pinch neck connective, and decapitate fly (*see* **Note 5**). Remove proboscis; carefully dissect away the cuticle, taking care not to rip delicate connective tissue between the central brain and the optic lobes.
2. Position brain posterior side down on the Sylgard, gently pushing it down so the posterior side of the brain sticks to the Sylgard (*see* **Note 3**).
3. Position one L-shaped micro-dissection pin over each optic lobe, inserting one side of the L-shape into Sylgard such that the other side of the L holds optic lobes down (*see* **Note 6**). Placing the pin in the space between the medulla and the lamina provides good stability, without interfering with access to the central brain. A slight amount of lateral stretch of the brain and the use of fresh Sylgard dishes will help keep the brain firmly affixed to the Sylgard (Fig. 1b).
4. Remove the perineuronal sheath overlying the antennal lobe (or other areas to be targeted for whole-cell recordings) using forceps [23]. Alternatively, the sheath can be digested using collagenase [25].

3.5 Perform Stimulation

We describe a protocol for stimulating antennal lobe projection neurons (PNs), but this strategy can be used for any cell type with good genetic and optical access:

1. Establish a whole-cell recording from a PN, in current clamp. This procedure has been described in detail by [18]. This is necessary for validation of optogenetic stimulation. Once validation has been performed, other neurons or behavioral measures can be monitored during stimulation.
2. Acquire an image stack of the ReaChR:mCitrine fluorescence throughout the antennal lobe with the laser tuned to a wavelength of 920 nm. Based on this imagery, define the regions of interest (ROIs) that should be stimulated. These regions should include the possible dendrite locations of the recorded neuron. In other words, for recordings from *GH146-Gal4*, the entire antennal lobe should be covered. We typically found that stimulating 7×7 μm squares in a raster scan pattern to be a good compromise between achieving effective activation (i.e., sustained spike rates up to ~70 Hz) and retaining spatial resolution across glomeruli (Fig. 2). Produce a text file containing a list of coordinates for these regions of interest. This file should be formatted to be interpretable by the software running the microscope. Because the excitation will spread out in the Z dimension, each stimulation region will actually be a volume, which we refer to as a voxel. In our experiments, we have found the voxel size to be ~$7 \times 7 \times 8$ μm [13].

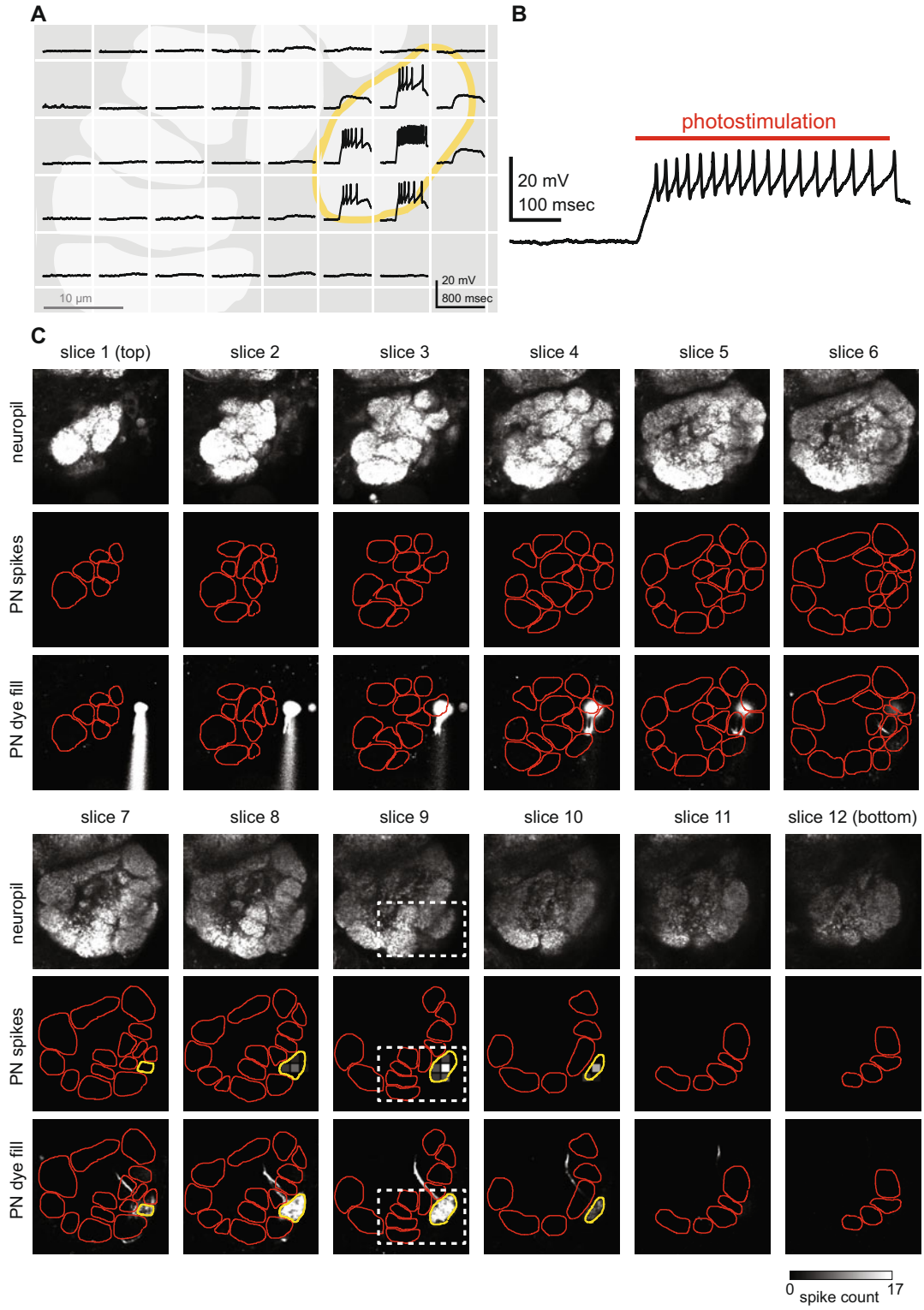

Fig. 2 Example of photostimulation of an antennal lobe PN recorded from an ex vivo preparation. (**a**) Summary of recorded membrane potential responses from a PN in response to photostimulation of several voxels. White lines denote the spatial arrangement of each voxel, and light gray shapes depict the borders of each

3. Load the ROI coordinate list into ScanImage using the photostimulation module (*see* **Note 7**).
4. Define duration and parameters of stimulation using ScanImage photostimulation module. We have found 250 ms of baseline recording followed by ~500 ms of stimulation to be useful. These durations are sufficient to make the detection of postsynaptic responses above baseline membrane potential fluctuations statistically distinguishable, even with just single stimulation trials. We raster scan each 7×7 μm square with 2 ms line durations and 8 lines, repeated 30 times (*see* **Note 8**). If particularly subtle responses to stimulation are expected, the total stimulation duration can be increased. In addition, stimulation can be performed in multiple trials and responses averaged.
5. Tune the laser to a wavelength of 1040 nm (*see* **Note 9**) and begin stimulation of ROIs (*see* **Note 10**). Simultaneously monitor and record the PN with patch-clamp recording. Synchronization of stimulation and recording can be achieved by triggering the ScanImage photostimulation module with the same hardware used to control physiology.
6. Periodically readjust the brain position, if necessary, by comparing current brain position to the image stack acquired on **step 2** of this section (*see* **Note 11**). Microscope and brain drift should be minimized by optimizing the equipment and dissections. However, in our experience there always remains unavoidable drift that is large enough to contaminate results, so periodic corrections are necessary.
7. After all ROIs have been stimulated, examine the PN recording to determine whether laser power is appropriate to drive spikes with glomerular precision. We attenuate the laser power to 3.0 mW (measured after the objective), which typically generates ~15 spikes per second, but occasionally can produce rates as high as 60–70 spikes per second. An example of PN

Fig. 2 (continued) glomerulus in this field of view. Black traces are the voltage responses of the PN to stimulation of each voxel. Only voxels that include the glomerulus outlined in yellow evoke spikes upon stimulation. (**b**) Detail of spiking activity in the PN in response to photostimulation. The laser is raster scanned to cover a complete voxel. This pattern is repeated 30 times within the 500 ms photostimulation period. Even though the raster scan is repeated, the PN's excitation is effectively continuous. (**c**) Twelve representative optical slices through the antennal lobe (each separated by 6 μm). For all slices, the top images display the neuropil stained with α-bungarotoxin (showing glomeruli). The middle images depict spike counts evoked by stimulation of each voxel (heatmap color scale in lower right). Yellow outline corresponds to the home glomerulus of the recorded PN in this experiment (same as panel **a**). Red outlines depict other glomeruli visible in each section. The bottom images depict the morphology of the PN. The dye-filled pipette is visible in slices 1–3 and the dye-filled cell body can be seen in slices 1–5. The dashed white rectangle in slice 9 corresponds to the field of view shown in (**a**). (Figure is reproduced from [13] and used with permission from Elsevier)

responses to stimulated ROIs throughout the antennal lobe is given in Fig. 2. Remember that increasing the light power to the specimen may reduce the spatial resolution of stimulation.

8. Adjust parameters as necessary (e.g., laser power attenuation; stimulation voxel size, shape, and pattern; stimulation duration) to meet spatiotemporal resolution needs. Stimulation efficiency will vary across preparations and targets. Confirm resolution needs are met for the population of desired targets on average by performing multiple experiments and sampling from the targets randomly.
9. When stimulation is over, acquire another image stack of the ReaChR:mCitrine fluorescence throughout the antennal lobe (at 920 nm) to document lack of drift.
10. Bathe the preparation in 10 μL of the 116 solution of μM α-bungarotoxin conjugated to Alexa Fluor 488 for 30 min. During this time, turn off any saline superfusion.
11. Wash out the excess α-bungarotoxin solution and acquire a final image stack of the Alexa Fluor 488 fluorescence throughout the antennal lobe (at a wavelength of 775 nm) at high spatial resolution for identification of stimulated neuropils (*see* **Note 12**).
12. Fix brain in 4% formaldehyde and save for immunohistochemistry against biocytin and nc82 for additional documentation of the morphology of recorded neuron.

The stimulation parameters are now set appropriately. This method can now be used simultaneously with recordings from other cells, behavioral measurements, or other readouts. For example, postsynaptic responses can be measured in lateral horn neurons during stimulation of PNs in the antennal lobe (Fig. 3).

4 Notes

1. Supplementing standard cornmeal agar fly food with rehydrated potato flakes (e.g., Formula 4-24 Instant *Drosophila* medium) can help the ATR solution absorb and distribute throughout the top of the vial. Alternatively, the cornmeal agar can be melted in a microwave and the ATR thoroughly mixed in.
2. An additional Sylgard "wedge" can also be prepared to tilt the brain up. This can be helpful for accessing cell bodies located on the dorsal and posterior side of the brain. The wedge can be cut from fresh Sylgard using a sharp needle and placed on the surface of a fresh Sylgard dish.

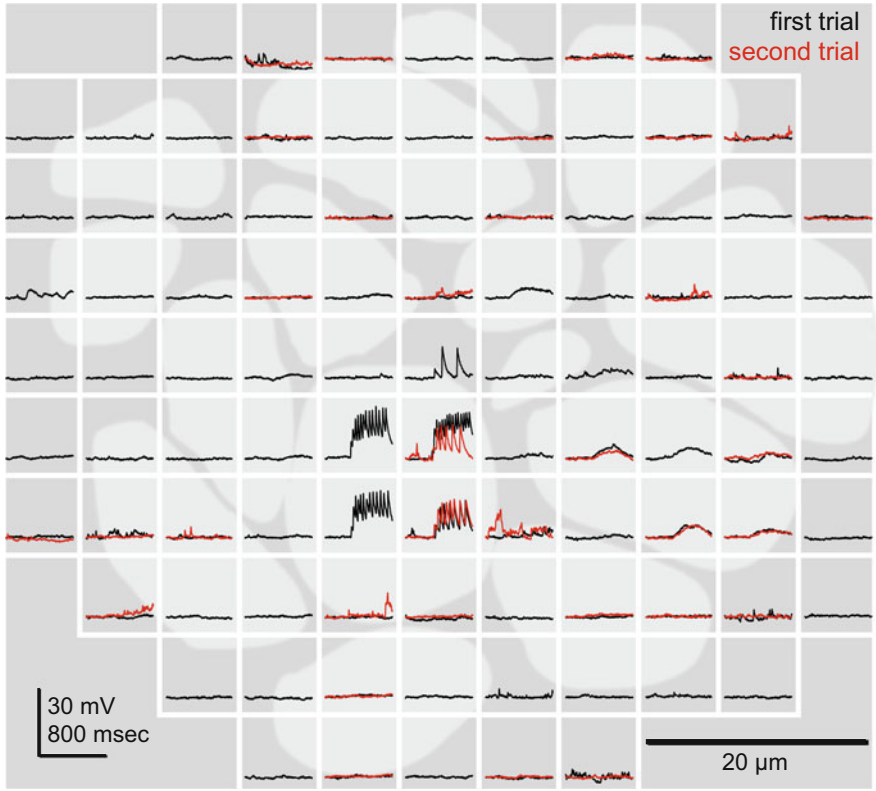

Fig. 3 Example of synaptic responses in a lateral horn neuron (LHN) to two-photon optogenetic stimulation of PNs, showing reliability of stimulation and response. LHN responses to photostimulation of every voxel in an entire z-plane. Responses are displayed within the corresponding voxel, with glomerular areas shown in pale gray. After stimulating all voxels (across all z-planes) once, roughly half of the voxels were stimulated again. Voxels that were repeatedly stimulated showed similar responses in this LHN (compare red and black traces). Note that the large responses in the center (corresponding to photostimulation of glomerulus VA6) consist of large EPSPs that do not evoke spikes. (Figure is reproduced from [13] and used with permission from Elsevier)

3. Use new and clean Sylgard dishes as often as possible. We prefer a new dish for every preparation. In our experience, the Sylgard loses its "stickiness" after several attempts at sticking a brain to it. If the brain is not sticking well, try replacing the Sylgard dish. Neural tissue adheres better to clean Sylgard which will make dissection easier.
4. Because imaging and stimulation occur at different wavelengths, the alignment of imaging and stimulation planes in the Z dimension can be distorted due to chromatic aberration. Imaging fluorescent microspheres at each wavelength will quantify this effect and enable compensatory analysis steps to be taken.

5. Fly cuticle is hydrophobic and thus it can be initially hard to keep intact flies in place for performing the initial dissection to remove the brain from the head capsule. Thus, we often perform our initial removal of the brain with the fly waxed into an in vivo fly holder [23].
6. Tungsten micro-dissection pins are tiny and can be easily lost. It is helpful to have several backup pins in case one disappears during the preparation.
7. Loading large numbers of photostimulation patterns into ScanImage manually can be tedious. We recommend using the ScanImage API to do this programmatically.
8. Repeated raster scanning stimulation works well because the activation and inactivation kinetics of ReaChR are relatively slow. As long as the scan pattern is fast enough, the neuron will achieve effectively continuous excitation.
9. We have found that 1040 nm works well for exciting antennal lobe PNs. However, the two-photon cross section of ReaChR peaks around 1000 nm [26]. We recommend testing several wavelengths to find which works best in each type of preparation.
10. Be sure to blank the laser during the inter-stimulation intervals, since any stray excitation light can cause unintended activation. In addition to fully attenuating the laser, we also "park" the scan mirrors such that any residual excitation light is directed far away from any neurons expressing the optogenetic actuator.
11. We recommend checking the brain position every ~15 min using a single fiduciary Z plane ~30 μm deep into the antennal lobe.
12. If you have added Alexa Fluor 568 to your pipette, the intracellular dye fill can be imaged on a second PMT channel of the microscope.

Acknowledgments

The authors gratefully acknowledge the support of Rachel Wilson in developing and refining this methodology. Kristyn Lizbinski provided critical feedback on the manuscript. This work was supported by NIH grants R01DC008174, F32NS083262, and P30NS072030, Yale University, and the Kavli Institute for Neuroscience at Yale.

References

1. Yizhar O, Fenno LE, Davidson TJ, Mogri M, Deisseroth K (2011) Optogenetics in neural systems. Neuron 71:9–34
2. Helmchen F, Denk W (2005) Deep tissue two-photon microscopy. Nat Methods 2:932–940
3. Rickgauer JP, Tank DW (2009) Two-photon excitation of channelrhodopsin-2 at saturation. Proc Natl Acad Sci U S A 106:15025–15030
4. Andrasfalvy BK, Zemelman BV, Tang J, Vaziri A (2010) Two-photon single-cell optogenetic control of neuronal activity by sculpted light. Proc Natl Acad Sci U S A 107:11981–11986
5. Mardinly AR, Oldenburg IA, Pegard NC, Sridharan S, Lyall EH, Chesnov K et al (2018) Precise multimodal optical control of neural ensemble activity. Nat Neurosci 21:881–893
6. Klapoetke NC, Murata Y, Kim SS, Pulver SR, Birdsey-Benson A, Cho YK et al (2014) Independent optical excitation of distinct neural populations. Nat Methods 11:338–346
7. Hernandez O, Papagiakoumou E, Tanese D, Fidelin K, Wyart C, Emiliani V (2016) Three-dimensional spatiotemporal focusing of holographic patterns. Nat Commun 7:11928
8. Zhang Z, Russell LE, Packer AM, Gauld OM, Hausser M (2018) Closed-loop all-optical interrogation of neural circuits in vivo. Nat Methods 15:1037–1040
9. Kazama H (2015) Systems neuroscience in Drosophila: conceptual and technical advantages. Neuroscience 296:3–14
10. Ito K, Shinomiya K, Ito M, Armstrong JD, Boyan G, Hartenstein V et al (2014) A systematic nomenclature for the insect brain. Neuron 81:755–765
11. Gouwens NW, Wilson RI (2009) Signal propagation in Drosophila central neurons. J Neurosci 29:6239–6249
12. Jenett A, Rubin GM, Ngo TT, Shepherd D, Murphy C, Dionne H et al (2012) A GAL4-driver line resource for Drosophila neurobiology. Cell Rep 2:991–1001
13. Jeanne JM, Fisek M, Wilson RI (2018) The organization of projections from olfactory glomeruli onto higher-order neurons. Neuron 98:1198–1213
14. Inada K, Tsuchimoto Y, Kazama H (2017) Origins of cell-type-specific olfactory processing in the drosophila mushroom body circuit. Neuron 95:357–367.e354
15. Kim SS, Rouault H, Druckmann S, Jayaraman V (2017) Ring attractor dynamics in the Drosophila central brain. Science 356:849–853
16. Takagi S, Cocanougher BT, Niki S, Miyamoto D, Kohsaka H, Kazama H et al (2017) Divergent connectivity of homologous command-like neurons mediates segment-specific touch responses in Drosophila. Neuron 96:1373–1387.e1376
17. Hsiao PY, Tsai CL, Chen MC, Lin YY, Yang SD, Chiang AS (2015) Non-invasive manipulation of Drosophila behavior by two-photon excited red-activatable channelrhodopsin. Biomed Opt Express 6:4344–4352
18. Murthy M, Turner G (2013) Whole-cell in vivo patch-clamp recordings in the Drosophila brain. Cold Spring Harb Protoc 2013:140–148
19. Pologruto TA, Sabatini BL, Svoboda K (2003) ScanImage: flexible software for operating laser scanning microscopes. Biomed Eng Online 2:13
20. Lin JY, Knutsen PM, Muller A, Kleinfeld D, Tsien RY (2013) ReaChR: a red-shifted variant of channelrhodopsin enables deep transcranial optogenetic excitation. Nat Neurosci 16:1499–1508
21. Inagaki HK, Jung Y, Hoopfer ED, Wong AM, Mishra N, Lin JY et al (2014) Optogenetic control of Drosophila using a red-shifted channelrhodopsin reveals experience-dependent influences on courtship. Nat Methods 11:325–332
22. Stocker RF, Heimbeck G, Gendre N, de Belle JS (1997) Neuroblast ablation in Drosophila P [GAL4] lines reveals origins of olfactory interneurons. J Neurobiol 32:443–456
23. Murthy M, Turner G (2013) Dissection of the head cuticle and sheath of living flies for whole-cell patch-clamp recordings in the brain. Cold Spring Harb Protoc 2013:134–139
24. Brady J (1965) A simple technique for making very fine, durable dissecting needles by sharpening tungsten wire electrolytically. Bull World Health Organ 32:143–144
25. Maimon G, Straw AD, Dickinson MH (2010) Active flight increases the gain of visual motion processing in Drosophila. Nat Neurosci 13:393–399
26. Chaigneau E, Ronzitti E, Gajowa MA, Soler-Llavina GJ, Tanese D, Brureau AY et al (2016) Two-photon holographic stimulation of ReaChR. Front Cell Neurosci 10:234